TOXICOLOGICAL SCIENCES **127(2)**, 382–390 (2012)
doi:10.1093/toxsci/kfs134
Advance Access publication April 5, 2012

Targets and Intracellular Signaling Mechanisms for Deoxynivalenol-Induced Ribosomal RNA Cleavage

Kaiyu He,*,† Hui-Ren Zhou,‡ and James J. Pestka*,†,‡,[1]

Department of Microbiology and Molecular Genetics; †Center for Integrative Toxicology; and ‡Department of Food Science and Human Nutrition, Michigan State University, East Lansing, Michigan 48824

[1]To whom correspondence should be addressed at Department of Food Science and Human Nutrition, Michigan State University, 234 Trout Food Science Building, 469 Wilson Road, East Lansing, MI 48824-1224. Fax: (517) 353-8963. E-mail: pestka@msu.edu.

Received February 7, 2012; accepted March 21, 2012

The trichothecene mycotoxin deoxynivalenol (DON), a known translational inhibitor, induces ribosomal RNA (rRNA) cleavage. Here, we characterized this process relative to (1) specific 18S and 28S ribosomal RNA cleavage sites and (2) identity of specific upstream signaling elements in this pathway. Capillary electrophoresis indicated that DON at concentrations as low as 200 ng/ml evoked selective rRNA cleavage after 6 h and that 1000 ng/ml caused cleavage within 2 h. Northern blot analysis revealed that DON exposure induced six rRNA cleavage fragments from 28S rRNA and five fragments from 18S rRNA. When selective kinase inhibitors were used to identify potential upstream signals, RNA-activated protein kinase (PKR), hematopoietic cell kinase (Hck), and p38 were found to be required for rRNA cleavage, whereas c-Jun N-terminal kinase and extracellular signal-regulated kinase were not. Furthermore, rRNA fragmentation was suppressed by the p53 inhibitors pifithrin-α and pifithrin-μ as well as the pan caspase inhibitor Z-VAD-FMK. Concurrent apoptosis was confirmed by acridine orange/ethidium bromide staining and flow cytometry. DON activated caspases 3, 8, and 9, thus suggesting the possible coinvolvement of both extrinsic and intrinsic apoptotic pathways in rRNA cleavage. Satratoxin G (SG), anisomycin, and ricin also induced specific rRNA cleavage profiles identical to those of DON, suggesting that ribotoxins might share a conserved rRNA cleavage mechanism. Taken together, DON-induced rRNA cleavage is likely to be closely linked to apoptosis activation and appears to involve the sequential activation of PKR/Hck → p38 → p53 → caspase 8/9 → caspase 3.

Key Words: **signal transduction; Gene Expression/Regulation; macrophage; Immunotoxicology; kinase.**

The trichothecenes, a group of sesquiterpenoid mycotoxins produced by *Fusarium* that contaminate wheat, barley, and corn globally, are problematic because of their resistance to degradation during processing and their potential to adversely affect human and animal health (Pestka, 2010). Among the over 200 trichothecenes discovered to date, deoxynivalenol (DON) is most frequently encountered in food, and human exposure to this toxin throughout the world has been well documented in a recent series of elegant biomarker studies (Hepworth *et al.*, 2012; Turner *et al.*, 2010a,b, 2011). A potential target for adverse health effects for DON is the innate immune system, with low doses of the toxin having immunostimulatory effects and high doses causing immunosuppression (Pestka, 2010).

At the mechanistic level, DON has been shown *in vitro* and *in vivo* to activate mitogen-activated protein kinases (MAPKs), including p38, c-Jun N-terminal kinase (JNK), and extracellular signal-regulated kinase (ERK) in macrophages and monocytes (Islam *et al.* 2006; Shifrin and Anderson, 1999; Zhou *et al.*, 2003a). These MAPKs mediate upregulation of proinflammatory cytokine and chemokine expression as well as apoptosis (Chung *et al.*, 2003; Islam *et al.*, 2006; Moon and Pestka, 2002). Notably, DON concentration dependently induces competing survival (ERK/AKT/p90Rsk/Bad) and apoptotic (p38/p53/Bax/mitochondria/caspase-3) pathways in the macrophage (Zhou *et al.*, 2005a). Accordingly, MAPK activation is critical to both stimulation and suppression of the innate immune system.

Two signal transducers that have been identified to be upstream of DON-induced MAPK activation are double-stranded RNA- (dsRNA) activated protein kinase (PKR) (Zhou *et al.*, 2003b) and hematopoietic cell kinase (Hck) (Zhou *et al.*, 2005b). PKR is a widely distributed constitutively expressed serine/threonine protein kinase that can be activated by dsRNA, interferon, proinflammatory stimuli, cytokines, and oxidative stress (Garcia *et al.*, 2006; Williams, 2001). PKR also activates p53, p38, JNK, Nuclear Factor-kappaB, signal transducer and activator of transcription, and interferon regulatory factor-1 (Williams, 1999). Hck, a member of Src kinase family, is expressed specifically in myelomonocytic cell lineages and transduces extracellular signals that regulate proliferation, differentiation, and migration (Ernst *et al.*, 2002; Tsygankov, 2003). Upon DON exposure, both PKR and Hck are activated prior to the MAPKs and their respective inhibitors suppress downstream MAPK activation (Zhou *et al.*, 2005b). Although crosstalk between PKR and Hck is not clearly

understood, PKR appears to be required for Hck interaction with the ribosome in the human monocyte U937 cell line (Bae *et al*., 2010).

A prominent consequence of DON exposure in macrophages is ribosomal RNA (rRNA) cleavage, which could negatively impact innate immune function (Li and Pestka, 2008). Two fundamental questions arising from this work relate to the specificity and mechanisms for this cleavage. Using oligonucleotide extension, we identified one site of DON-induced rRNA cleavage is within the peptidyl transferase center of 28S rRNA; however, further identification of additional sites was precluded by the relatively poor resolution of conventional gel electrophoresis and limitations on this techniques imposed by RNA hairpin structures (Li and Pestka, 2008). Regarding mechanisms, it is known that ricin and other ribosome-inactivating proteins (RIPs) cleave rRNA via a highly specific mechanism that involves *N*-glycosidase-mediated adenine depurination at highly conserved sarin/ricin (S/R) loop (Endo and Tsurugi, 1986; Hartley and Lord, 2004). However, DON and other trichothecenes are low molecular weight chemicals and are devoid of inherent enzyme activities (Li and Pestka, 2008). Induction of rRNA cleavage by chemicals or viruses has previously been suggested to be linked to apoptosis (Banerjee *et al*., 2000; Naito *et al*., 2009) raising the possibility that DON-induced rRNA cleavage might be similarly linked to this mechanism of cell death.

The purpose of this study was to characterize DON-induced rRNA fragmentation with respect to (1) specific sites of 18S and 28S rRNA cleavage and (2) identity of upstream signaling events that mediate this process. The results demonstrate that DON promotes cleavage of 18S rRNA and 28S rRNA into a minimum of five and six fragments, respectively. Furthermore, DON-induced rRNA cleavage occurred concurrently with apoptosis was mediated by sequential activation of PKR, Hck, p38, p53, and several caspases. Three other translational inhibitors, satratoxin G (SG), anisomycin, and ricin, evoked comparable selective rRNA cleavage to DON, suggesting that a common mechanism might exist for other ribotoxins.

MATERIALS AND METHODS

Chemicals. DON, anisomycin, PKR inhibitor C-16, and Hck inhibitor PP1 were purchased from Sigma-Aldrich (St Louis, MO). Ricin was obtained from Vector Labs Inc. (Burlingame, CA). SG was purified as described previously (Islam *et al*., 2009). The p38 inhibitor SB 203580, JNK inhibitor SP600125, ERK inhibitor PD 98059, RNase L Activator, p53 inhibitor pifithrin-α, and pifithrin-μ were purchased from EMD Chemicals Inc. (Gibbstown, NJ). Pan caspase inhibitor Z-VAD-FMK was supplied by BD Biosciences (San Diego, CA). [γ-^{32}P]ATP was purchased from PerkinElmer. All other chemicals and media components were obtained from Sigma-Aldrich, except where noted.

Cell culture. RAW 264.7 cells (ATCC, Rockville, MD) were cultured in Dulbecco's modified Eagle's medium supplemented with 10% (vol/vol) heat-inactivated fetal bovine serum (Atlanta Biologicals, Lawrenceville, GA), streptomycin (100 μg/ml), and penicillin (100 U/ml) at 37°C in a humidified incubator with 5% CO_2. Cell number and viability were assessed by trypan blue dye exclusion using a hematocytometer. Prior to exposure of toxins (DON, SG, anisomycin, and ricin) or inhibitors, cells (2.5×10^6) were seeded and cultured in 100-mm tissue culture plates for 24 h to achieve approximately 80% confluency.

RNA purification and fragmentation analysis. RNAs were extracted by TRIZOL (Invitrogen, Carlsbad, CA) following the manufacturer's protocol and their concentrations were measured using a NanoDrop reader (ThermoFisher, Wilmington, DE). Fragmentation of RNA was assessed by denaturing agarose gel electrophoresis (Li and Pestka, 2008) or capillary electrophoresis using an Agilent 2100 Bioanalyzer with a NanoChip (Agilent, Santa Clara, CA) according to manufacturer's instructions.

Northern blot analysis. Northern blot analysis was performed by a modification of a previously described procedure (Li and Pestka, 2008). Briefly, probes (Table 1) were labeled with γ-^{32}P by DNA 5′ end-labeling system (Promega, Madison, WI) and purified by Micro-Bio-Spin6 chromatography column (Bio-Rad, Hercules, CA). Label incorporation was measured using a TopCount NXT (PerkinElmer, Shelton, CT). Total RNA (10 μg per lane) was separated on a 1.2% (wt/vol) formaldehyde denaturing agarose gel and transferred to a Biodyne membrane (Pall Gelman Laboratory, Ann Arbor, MI). After ultraviolet (UV) crosslinking (Stratagene, Cedar Creek, TX), membranes containing immobilized RNA were prehybridized for 1 h at 68°C and then incubated with [γ-^{32}P]-labeled probes (1×10^6 cpm/ml) in Quickhyb solution (Stratagene) containing 200 μg/ml of herring sperm DNA at 68°C for 2 h. Blots were washed twice with 2× Side Scatter (SSC) containing 0.1% (wt/vol) SDS at room temperature and once for 15 min with 0.1× SSC containing 0.1% (wt/vol) SDS at 50°C. The membranes were assembled with the Hyblot autoradiography film (Denville, Metuchen, NJ) into an X-ray exposure cassette and the film was developed after 24 h.

Immunoblotting. Western blot analyses were conducted using primary antibodies specific for murine forms of total/cleaved caspase 9, cleaved caspase 3 (Asp 175), total caspase 8, and cleaved caspase 8 (Asp387) (Cell Signaling, Beverly, MA). Mouse β-actin antibody (Sigma) was also used to verify equal loading. Cells were washed twice with ice-cold phosphate-buffered saline (PBS), lysed in boiling lysis buffer (1% [wt/vol] SDS, 1 mM sodium orthovanadate, and 10 mM Tris, pH 7.4), boiled for 5 min, and sonicated briefly, the resultant lysate centrifuged at 12,000 × g for 10 min at 4°C and protein concentration measured with a BCA Protein Assay Kit (ThermoFisher, Pittsburgh, PA). Total cellular proteins (40 μg) were separated on Bio-Rad precast 4–20% polyacrylamide gels (Bio-Rad) and transferred to a polyvinylidene difluoride membrane (Amersham, Arlington Heights, IL). After incubating with blocking buffer (Li-Cor, Lincoln, NE) for 1 h at 25°C, membranes were incubated with murine and/or rabbit primary antibodies (1:1000 dilution in Li-Cor blocking buffer) to immobilized proteins of interest overnight at 4°C. Blots were washed three times of 10 min with Tris-buffered saline and Tween 20 (50 mM Tris-HCl, 150 mM NaCl, and 0.1% Tween 20, pH 7.5) and then incubated with secondary IRDye 680 goat anti-rabbit and/or IRDye 800CW goat anti-mouse IgG antibodies (Li-Cor) (1:2000 dilution in Li-Cor blocking buffer) for 1 h at 25°C. After washing three times, infrared fluorescence from these two antibody conjugates were simultaneously measured using a Li-Cor Odyssey Infrared Imaging System.

Apoptosis measurement by acridine orange/ethidium bromide staining. Acridine orange/ethidium bromide (AO/EB) staining was carried out using an adaptation of a previously described procedure (Muppidi *et al*., 2004). Briefly, slides were cleaned and sterilized by UV light, placed into 100-mm tissue culture plates, and cultured with RAW 264.7 cells (2.5×10^6) for 24 h to achieve approximately 80% confluency. DON-exposed RAW 264.7 cells were stained for 2 min with 100 μg/ml AO and 100 μg/ml EB in PBS. The slides were washed twice with cold PBS and then covered with coverslip and examined at ×400 under Nikon fluorescence microscope equipped with a wide-band fluorescein isothiocyanate filter. Cells ($\geq$ 200) were classified based on their nuclear morphology (bright chromatin, highly condensed, or fragmented nuclei) in to four categories: viable normal (VN),

TABLE 1
18S and 28S rRNA Probes for Northern Blot Analysis of rRNA Cleavage[a]

Probe	Sequences	Position
28S Probe 1	5′-ACCCGGCGTTCGGTTCAT-3′	1,690–1,707
28S Probe 2	5′-AAAGGACGGGGGGTCTCCCCGG-3′	2,732–2,753
28S Probe 3	5′-GGGTTGGACCCGCCGCCCCGGAG-3′	2,877–2,899
28S Probe 4	5′-GCGGGCCTTCGCGATGCTTTGTT-3′	3,304–3,326
28S Probe 5	5′-ACCCAGAAGCAGGTCGTCTACGAATGGTTTAGCGCCAG-3′	4,605–4,642
18S Probe 1	5′-GCACCAGACTTGCCCTCC-3′	598–615
18S Probe 1	5′-GAATAAC GCCGCCGCATC-3′	1,100–1,117
18S Probe 1	5′-CGGA CATCTAAGGG CATCACAG-3′	1,493–1,514

[a]NCBI access numbers for 28S and 18S rRNA sequences are NR_003279 and NR_003278, respectively.

viable apoptotic (VA), nonviable apoptotic (NVA), and nonviable necrotic (NVN). The apoptotic index was calculated as follows: (VA + NVA)/(VN + VA + NVN + NVA) × 100.

Apoptosis measurement by flow cytometry. RAW 264.7 cells were treated with vehicle PBS or DON (1000 ng/ml) for 6 h. Total DON-treated cells and adherent DON-treated cells were collected separately. After washing twice with cold PBS, annexin staining was performed according to the manufacturer's protocol (BD Biosciences). Briefly, cells were resuspended to 1× binding buffer at a concentration of 2.5×10^6 cells/ml, and 100 μl of the cell suspension was transferred to fluorescence activated cell sorter tubes. Cells were incubated with 5 μl of annexin V and propidium iodide (PI) for 15 min at room temperature in dark. Finally, samples were resuspended to 400 μl volume with binding buffer, acquired on the Accuri C6 Flow Cytometer (Ann Arbor, MI), and analyzed using FlowJo software (Tree Star, Ashland, OR). Live Raw 264.7 cells were gated using Forward Scatter versus SSC.

Statistics. Data were analyzed by Student's *t*-test using Sigma Stat 3.11 (Jandel Scientific, San Rafael, CA). Data sets were considered significantly different when $p < 0.05$.

RESULTS

DON Induces rRNA Cleavage

The capacity of DON to induce rRNA cleavage in RAW 264.7 macrophages was assessed by denaturing gel electrophoresis (Fig. 1A) and capillary electrophoresis (Figs. 1B and 1C). Distinct 18S and 28S rRNA bands were evident in both control and DON-treated RAW 264.7 cells, whereas over five additional rRNA fragment bands were detected in DON-treated cells. Based on its high resolution and reproducibility as compared with conventional electrophoresis, capillary electrophoresis was employed to monitor cleavage in subsequent experiments. When the kinetics of the response were measured, DON at 1000 ng/ml was found to cause rRNA cleavage as early as 2 h that was very robust by 6 h (Figure 2A). Cleavage at 6 h was concentration dependent with 200 ng/ml of DON evoking modest rRNA cleavage as compared with more marked rRNA cleavage induced by 1000 ng/ml (Figure 2B). Based on these findings, incubation with DON at 1000 ng/ml for 6 h was uniformly employed for subsequent mechanistic studies.

DON Induces Cleavage of Both 28S and 18S rRNA

Northern blot analyses using ^{32}P-labeled oligonucleotide probes (Table 1) for 18S and 28S rRNAs were performed to identify and map sites of rRNA cleavage. Incubation with five probes complementary to 28S rRNA revealed six fragments (a–f) with sizes approximating 4000, 3200, 2800,

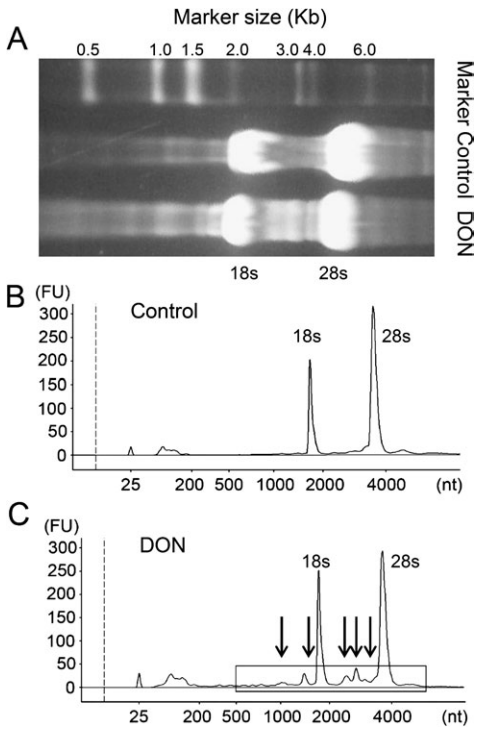

FIG. 1. Detection of DON-induced rRNA cleavage in RAW 264.7 by agarose gel and capillary electrophoresis. Cells were treated with or without 1000 ng/ml DON for 6 h. RNAs were purified and analyzed either (A) on 1.2% formaldehyde denaturing agarose gel (10 μg) or (B and C) by capillary electrophoresis (300 ng). The x-axis indicates the size of the fragments in nucleotide (nts) and the y-axis indicates the relative peak intensity in fluorescence units (FU). The two major peaks represent 18S rRNA (~2000 nts) and 28S rRNA (~4000 nts). Arrows designate three significant cleavage peaks between 28S and 18S rRNA and two peaks below 18S rRNA. Rectangle in C indicates chart region to be shown in subsequent figures.

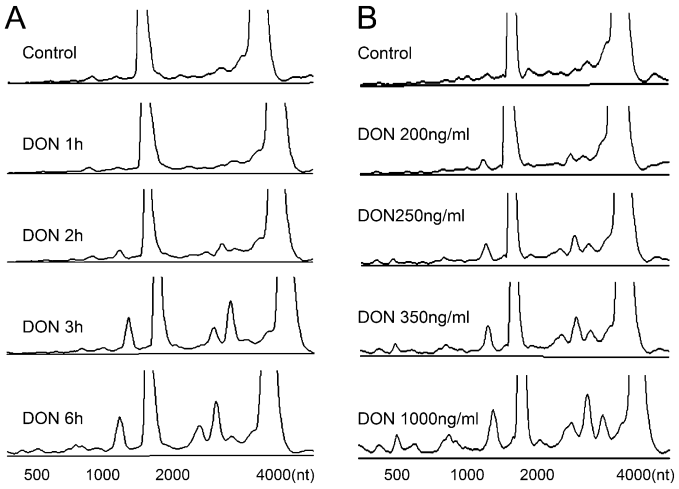

FIG. 2. Kinetics and concentration dependence of DON-induced rRNA cleavage in RAW 264.7. (A) Cells were treated with 1000 ng/ml DON at intervals and total RNAs were analyzed for cleavage by capillary electrophoresis. (B) RAW 264.7 cells were treated with indicated concentrations of DON for 6 h and total RNAs were purified and analyzed by capillary electrophoresis. Only the regions between 500 and 4000 nts are shown.

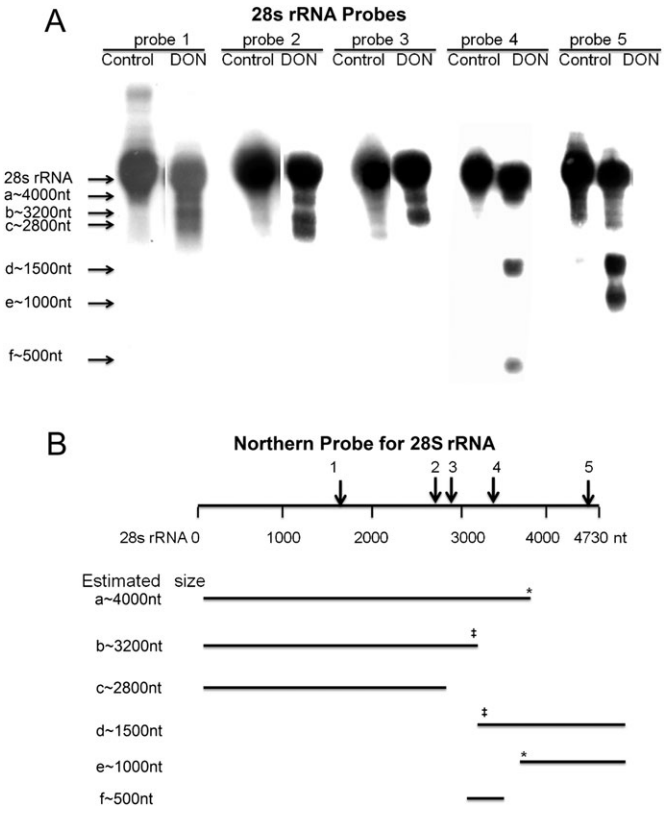

FIG. 3. Proposed 28S rRNA cleavage sites in RAW 264.7 based on Northern blot analysis. (A) Five probes complementary to 28S rRNA were hybridized to RNAs from RAW 264.7 cells treated with vehicle or DON (1000 ng/ml) for 6 h. Arrows indicate fragments from 28S rRNA identified by Northern blot analysis and their corresponding sizes (nts). Results are representative of three separate experiments. (B) Depiction of proposed 28S rRNA cleavage pattern. Fragments with same symbol (* and ‡) are likely to originate from the same intact 28S rRNA.

1500, 1000, and 500 nts (Fig. 3A). Based on rRNA fragment sizes, probe position and Northern blotting, putative cleavage sites of 28S rRNA were deduced (Figure 3B). DON appeared to cleave 28S rRNA into one of two pairs of fragments: a + e (approximately 5000 nts) and b + d (approximately 4700 nts). Because no complementary fragment (approximately 2000 nts) to fragment c was detected, it was likely to be a product of the subsequent degradation of a or b.

Autoradiography following hybridization with three probes complementary to 18S rRNA indicated the presence of five fragments (*A-E*) with approximate sizes of 1000, 800, 600, 500, and 300 nts (Fig. 4 A). The putative 18S rRNA cleavage pattern suggested that fragments A (approximately 1000 nts) and B (approximately 800 nts) are derived from intact 18S rRNA, whereas the remaining fragments (C, D, and E, approximately 600, 500, and 300 nts, respectively) resulted from further secondary cleavage of the two primary fragments (C and E from A and D from B) (Fig. 4B).

DON-induced rRNA Cleavage Is Concurrent With Apoptosis

AO/EB staining of adherent RAW 264.7 cells revealed that DON exposure (1000 ng/ml, 6 h) induced significant apoptosis concurrent with rRNA degradation (Fig. 5A). Because RAW 264.7 cells attach to the bottom of the cell culture plate under normal physiological conditions but detach during apoptosis, flow cytometry was additionally employed to measure apoptosis in adherent and suspended cells following DON treatment (Fig. 5B). Both adherent and total populations contained markedly higher annexin V-positive cells (early apoptotic) (60 and 78%, respectively) than the control total cells (31%). Similarly, the percentage of annexin V/PI-double positive cells (late apoptotic) were much higher in adherent (4.8%) and total (10.8%) populations than that of the control (1.2%).

DON-Induced rRNA Cleavage Requires PKR, Hck, p38, p53, and Caspase Activation

Because DON-induced apoptosis involves activation of PKR, Hck, and MAPKs (Zhou *et al.*, 2003b; Zhou *et al.*, 2005b), the role of these kinases in rRNA cleavage was determined using selective inhibitors. Both the PKR inhibitor C-16 (0.1 and 0.3 μM) (Fig. 6A) and the Hck inhibitor PP1 (5 and 25 μM) (Fig. 6B) were found to concentration dependently suppress DON-induced rRNA cleavage. Although the p38 inhibitor (SB 203580; 1 and 5 μM) also inhibited DON-induced rRNA cleavage concentration dependently (Fig. 6C), inhibitors of JNK (SP600125; 0.2, 1, and 5 μM) and ERK (PO 98059; 20 and 100 μM) did not (data not shown) have suppressive effects. Thus, as has been observed for DON-induced apoptosis, PKR, Hck, and p38 appeared to be key upstream elements for DON-induced rRNA cleavage.

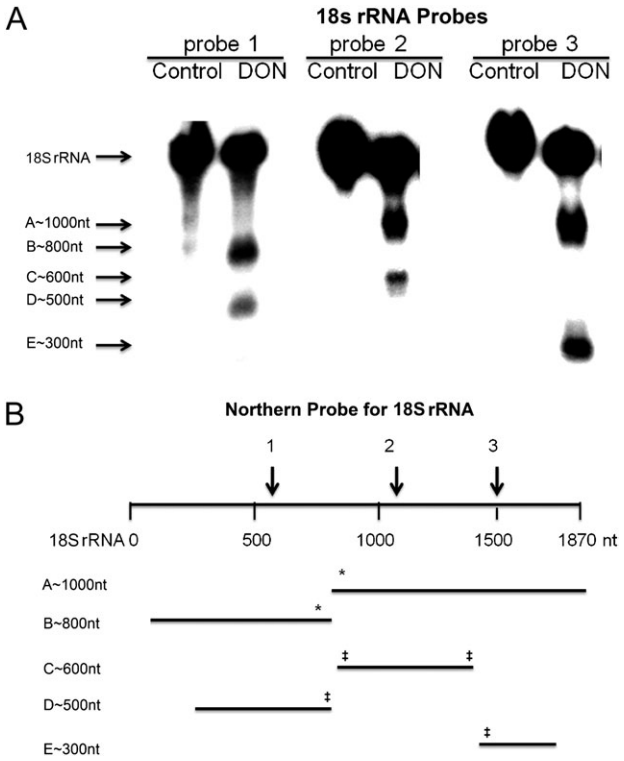

FIG. 4. Proposed 18S rRNA cleavage sites in RAW 264.7 based on Northern blot analysis. (A) Three probes complementary to 18S rRNA were hybridized to RNAs from RAW 264.7 cells treated with vehicle or DON (1000 ng/ml) for 6 h. Arrows indicate fragments from 18S rRNA identified by Northern blot analysis and their corresponding sizes (nts). Results are representative of three separate experiments. (B) Depiction of proposed cleavage pattern for 18S rRNA. Fragments with same symbol (* and ‡) are likely to originate from the same intact 18S rRNA.

It was previously shown that p38 mediates the sequential activation of p53 and caspase 3 to induce apoptosis in RAW 264.7 cells (Zhou *et al.*, 2005a). Suppression of DON-induced rRNA cleavage was observed here both for pifithrin-α (80 and 100 μM) (Fig. 6D), which can reversibly inhibit p53-dependent transactivation of p53-responsive genes and apoptosis and for pifithrin-μ (10 and 25 μM) (Fig. 6E), which blocks p53 interaction with Bcl-2 family proteins and selectively inhibits p53 translocation to mitochondria. The caspase inhibitor Z-VAD-FMK also caused concentration-dependent inhibition of DON-induced rRNA cleavage (Fig. 6F). Accordingly, both p53 and caspase activation are additional upstream elements in the signaling pathway leading to DON-induced rRNA cleavage.

Extrinsic and intrinsic apoptotic pathways activate caspase 3 through caspases 8 and 9, respectively. To discern possible contributions of these two pathways, RAW 264.7 cells were treated with DON for 3 and 6 h and the presence of cleaved caspases 8, 9, and 3 was determined by Western blot analysis. Cleavage of caspases 3, 8, and 9 was observed (Figs. 7A and 7B), suggesting that extrinsic and intrinsic pathways could potentially be involved in DON-induced rRNA fragmentation (Fig. 8).

SG, Anisomycin, and Ricin but Not Lipopolysaccharide Evoke rRNA Cleavages

Lipopolysaccharide, a major component of the outer membrane of Gram-negative bacteria that can activate macrophages via the Toll-like receptor 4 receptor, did not affect rRNA integrity indicating that the macrophage activation *per se* was insufficient to induce RNA cleavage. Because DON is a translational inhibitor and causes rRNA cleavage indirectly, we questioned whether this might be a common effect for other ribotoxins. Cells were incubated with SG and anisomycin, which can freely diffuse through cell membrane and ricin, a RIP, which can enter the cells by endocytosis and retrograde translocation to ER and cytosol. Unlike SG and anisomycin that directly bind to ribosome to inhibit translation, ricin possesses inherent RNA N-glycosidase activity to depurinate RNA. Although these toxins have apparently different mechanisms for inhibiting translation, SG, anisomycin, and ricin induced a similar apoptosis-mediated cleavage profile to that of DON (Fig. 8), suggesting that ribotoxins might share conserved pathway for mediating rRNA cleavage.

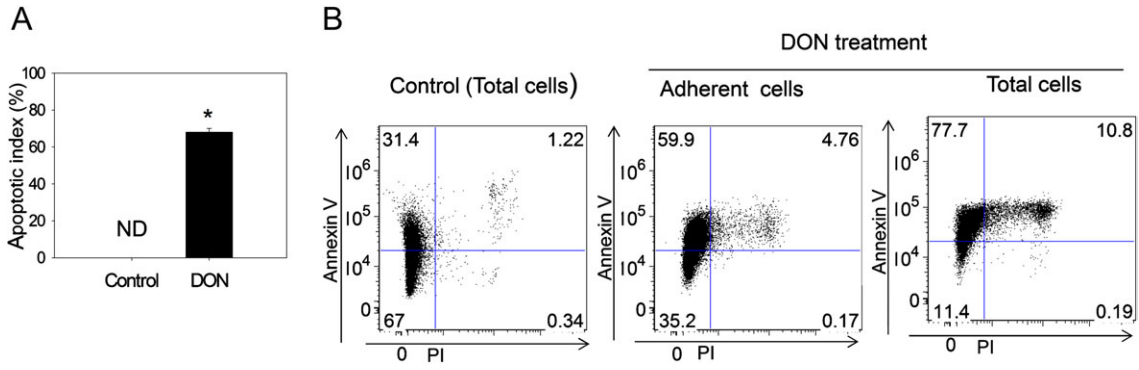

FIG. 5. DON exposure induces apoptosis in RAW 264.7. Cells were treated with DON (1000 ng/ml) for 6 h. (A) AO/EB was used to calculate apoptotic index in adherent cells. ND indicates nondetectable. Asterisk indicates statistically significant differences in cell apoptosis as compared with control ($p < 0.05$). (B) Flow cytometry with annexin V/PI was used to compare apoptosis in control and DON-treated adherent cells and total cells.

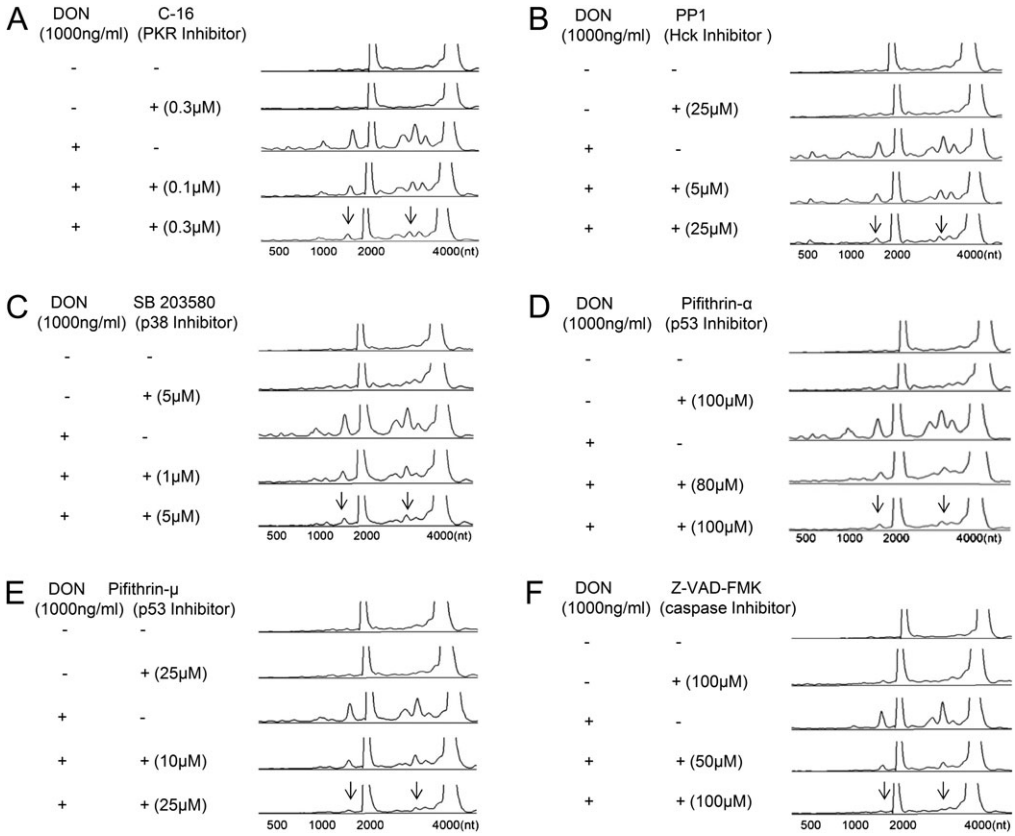

FIG. 6. DON-induced rRNA cleavage in RAW 264.7 involves PKR, Hck, p38, p53, and caspases. Cells were preincubated with (A) C-16 (0.1 or 0.3 μM), (B) PP1 (5 or 25 μM), (C) SB 203580 (1 or 5 μM), (D) pifithrin-α (80 or 100 μM), (E) pifithrin-μ (10 or 25 μM), or (F) Z-VAD-FMK (50 or 100 μM) for 1 h and then with DON (1000 ng/ml) for 6 h. RNAs were purified and analyzed by capillary electrophoresis. Results are representative of three separate experiments. Arrows indicate that fragmentation to major cleavage peaks is suppressed by inhibitor.

DISCUSSION

Understanding how DON induces rRNA degradation will provide insight into the mechanisms by which trichothecenes and other ribotoxins incapacitate or kill immunocompetent cells. The results presented here establish for the first time that (1) DON-induced cleavage at a limited number of sites in both 18S rRNA and 28S rRNA, (2) these cleavages result from PKR-driven p38 activation, (3) these events closely parallel induction of apoptosis by this mycotoxin, and (4) DON's effects are shared with other ribotoxic agents.

In higher eukaryotes, 28S rRNA contains 12 conserved but variable divergent domains (D1–D12), originating from evolutionary large-scale length and diversity expansions (Michot *et al.*, 1984). Although the functions of D domains are not clearly understood, D2 and D8 have higher divergency rates than other domains (Houge *et al.*, 1995). Mouse 28S rRNA cleavage sites have been mapped to be within D2 (approximately 400–1140 nts) and/or D8 domains (approximately 2700–3280 nts) (Houge *et al.*, 1993; Houge *et al.*, 1995; Houge and Doskeland, 1996; Naito *et al.*, 2009). Apoptosis-associated cleavage pathways were previously reported to target D2 and D8 followed by secondary cleavage in other domains. As demonstrated here, DON-induced rRNA cleavage fragments (b–f) were from the D8 region, whereas two other cleavage sites (a and e) were within D10 (approximately 3785–3822 nts) (Michot *et al.*, 1984) rather than canonical D2. It might be speculated that DON treatment rendered D8 and D10 accessible to constitutive and/or inducible RNases, whereas D2 did not.

We have previously reported that upregulated expression of several RNases in DON-treated RAW 264.7 cells occurs prior to or simultaneously with rRNA degradation (Li and Pestka, 2008). Particularly notable was RNase L, an enzyme that can mediate inhibition of protein synthesis, apoptosis induction, and antiviral activity (Stark *et al.*, 1998). Although RNase L is activated by a number of stressors, its only known endogenous direct activator is 2-5A, a product of oligoadenylate synthetase (Pandey *et al.*, 2004; Liang *et al.*, 2006). Upon binding to 2–5A, RNase L is activated by dimerization and possibly inhibits protein synthesis via the degradation of both messenger RNA and 28S rRNA (Clemens and Vaquero, 1978; Wreschner *et al.*, 1981). We found that under cell-free conditions in the presence of 2-5A, RNase L readily cleaved both FRET probe and purified rRNA; however, it did not degrade rRNA in

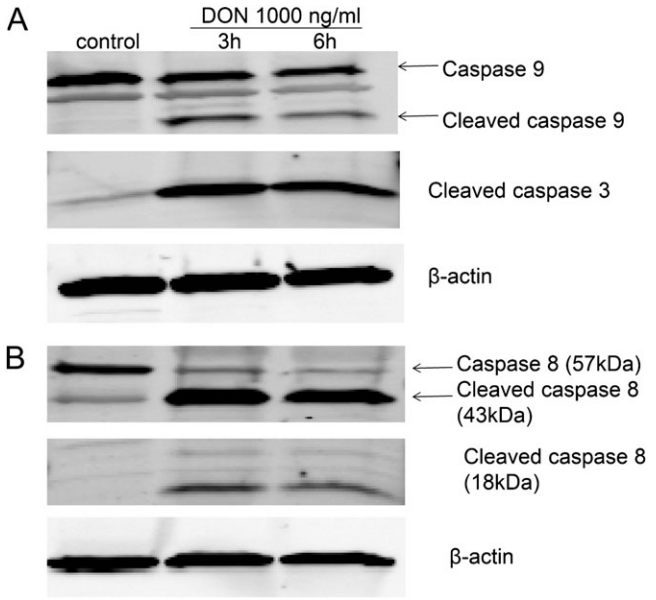

FIG. 7. DON induces cleavage of caspases 3, 8, and 9 in RAW 264.7. Cells were treated with DON (1000 ng/ml) for 3 and 6 h. Western blotting was used to detect (A) caspase 9, cleaved caspase 9, and cleaved caspase 3 and (B) caspase 8 and cleaved caspase 8. β-Actin was used as loading control. Data are representative of three separate experiments.

purified whole ribosomes (see supplementary fig. 1). Furthermore, transfection of 2-5A and RNase L activator (RLA) into RAW 264.7 cells did not induce rRNA cleavage. Thus, increased RNase L activity alone might likely be insufficient for inducing rRNA cleavage in RAW 264.7.

The observation that p38 but not JNK mediated DON-induced rRNA cleavage is consistent with previous observations that p38 is a central regulator of cell fate in DON-exposed macrophages (Zhou *et al.*, 2005a). Our findings further demonstrate that PKR and Hck also mediate DON-induced

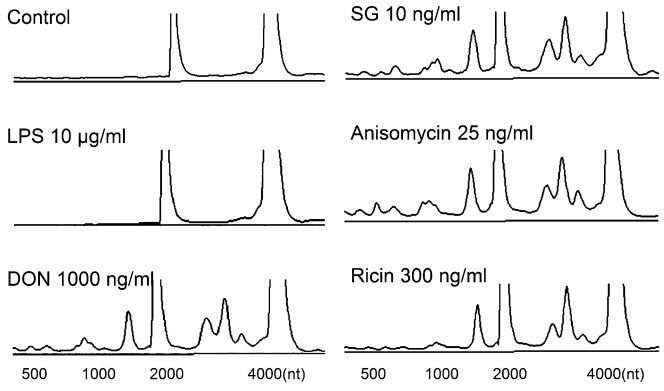

FIG. 8. SG, anisomycin, and ricin but not lipopolysaccharide induce rRNA cleavage patterns identical to DON in RAW 264.7. Cells were treated with DON (1000 ng/ml), SG (10 ng/ml), anisomycin (25 ng/ml), ricin (300 ng/ml), and lipopolysaccharide (10 μg/ml) for 6 h. RNAs were purified and analyzed by capillary electrophoresis. Results are representative of three separate experiments.

rRNA cleavage. Although crosstalk between PKR and Hck is still not completely understood, these kinases are well-established upstream mediators of DON-induced p38 activation (Zhou *et al.*, 2003b, 2005b). These data are consistent with our previous observations that 40S ribosome subunit-associated PKR, Hck, and p38 are activated upon DON exposure (Bae *et al.*, 2010).

We have previously hypothesized that rRNA cleavage might yield a double-stranded (ds) hairpin fragments capable of activating ribosome-associated PKR through its dsRNA-binding sites (Li and Pestka, 2008). The data presented here do not support this hypothesis. First, PKR and Hck are activated by DON within minutes (Zhou *et al.*, 2003b, 2005b), whereas DON-induced rRNA cleavage was detectable only after 2 h and required relatively higher DON concentrations. Second, suppression of DON-induced rRNA cleavage by PKR, Hck, and p38 inhibitors suggests that their activation is an upstream rather than downstream event. We therefore propose an alternative hypothesis in which entry of DON into the cell rapidly disrupts the conformation of rRNA yielding accessible intact hairpin loops at the surface of ribosome that would be capable of activating PKR or other double-stranded RNA–binding proteins. These events would initiate a stress response that would, especially at high toxin concentrations, ultimately drive rRNA cleavage in concert with apoptosis. This hypothesis is highly consistent with the growing recognition that damage-associated molecular patterns (DAMPs) initiate noninfectious innate immune and inflammatory responses (Newton and Dixit, 2012).

Bulavin *et al.* (1999) have previously shown that p38 mediates p53 phosphorylation. It was thus notable that rRNA cleavage was found here to be inhibited by pifithrin-α, a compound that reversibly inhibits both p53-dependent transactivation of p53-responsive genes and apoptosis, as well as by pifithrin-μ, which blocks p53 interaction with Bcl-2 family proteins and selectively inhibits p53 translocation to mitochondria. Relatedly, we have previously demonstrated that DON induces translocation of BAX (a member of Bcl-2 family) to mitochondria and release of cytochrome c leading to apoptosis (Zhou *et al.*, 2005a). Finally, DON-induced rRNA cleavage was completely suppressed by the pan caspase inhibitor Z-VAD-FMK, indicating that activation of caspases was a prerequisite of rRNA cleavage.

Caspases, proteolytic enzymes that play important roles in inflammation and cell death, are independently activated via either an intrinsic pathway involving caspase 9 or an extrinsic pathway through caspase 8 (Fuentes-Prior and Salvesen, 2004). It is thus important to note that DON activated caspases 8 and 9, both of which can activate caspase 3, suggesting the involvement of both apoptotic pathways, respectively, in rRNA cleavage. Caspases mediate degradation of some ribosomal-associated proteins, including eukaryotic translation initiation factor (eIF)2α, eIF3/p35, eIF4B, and eIF4G family (Clemens *et al.*, 2000). This proteolytic action might expose ribosome-

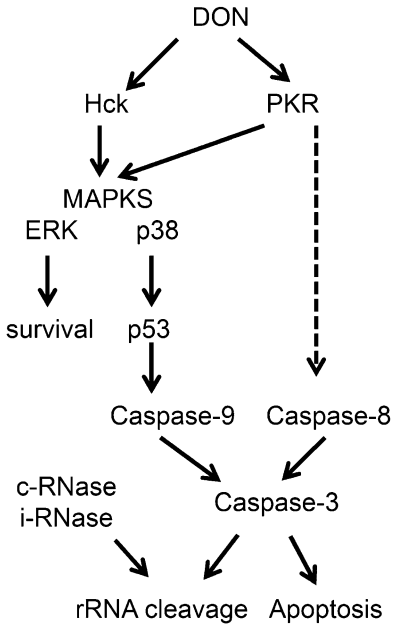

FIG. 9. Model for DON-induced rRNA cleavage. Figure depicts putative signaling pathways for induction of rRNA cleavage by DON. DON sequentially activates PKR/Hck, p38, p53, and caspase 9/3 leading to apoptosis-associated rRNA cleavage. Caspase 8 might also be concurrently activated by PKR further contributing to caspase 3-mediated apoptosis-associated rRNA cleavage. Note both constitutive (c) and inducible (i) RNases might contribute to the cleavage of rRNA exposed by caspase action.

embedded rRNA to constitutive and inducible RNases, resulting in the highly selective cleavage observed here.

The DON concentrations used in this study (200–1000 ng/ml) are consistent with those predicted to be in plasma and tissues (e.g., spleen, liver, and small intestine) of mice treated with immunosuppressive doses ($\geq$ 2 mg/kg bw) of this toxin (Azcona-Olivera *et al*., 1995; Li *et al*., 2005, 2007). Turner *et al*. (2010) estimated daily intake of DON in male Normandy farmers to range between 27 and 1088 ng/kg/day. Thus, the concentrations employed in the present study might only likely be encountered in humans that have consumed a large bolus dose of DON in a heavily contaminated cereal.

The results presented here and previously demonstrate that DON-induced rRNA cleavage requires prior sequential activation of PKR/Hck, p38, p53, and caspases (Fig. 9). It was remarkable that ricin, which possesses *N*-glycosidase enzymatic activity for 28S rRNA depurination, induced the identical rRNA cleavage profile to that of DON and two other low molecular weight translational inhibitors, SG and anisomycin. Possibly, in all four cases, toxin-mediated ribosome damage activated a canonical apoptosis-associated rRNA cleavage pathway. Future work should focus on understanding how DON mediates PKR activation, identifying critical executing caspases and RNases, ascertaining whether induction of rRNA cleavage by other ribotoxins or apoptosis-inducing agents is mediated by the same intracellular signaling pathways as well as validating these findings in animal models.

SUPPLEMENTARY DATA

Supplementary data are available online at http://toxsci.oxfordjournals.org/.

FUNDING

National Institutes of Health (PHS grant ES003358); United States Department of Agriculture (grant 59-0206-9-058).

ACKNOWLEDGMENTS

We thank Babal K. Jha, Robert H. Silverman, Mary Rosner, Eleni Beli, Laura Vines, and Brenna Flannery for technical assistance, advice, and suggestions.

REFERENCES

Azcona-Olivera, J. I., Ouyang, Y., Murtha, J., Chu, F. S., and Pestka, J. J. (1995). Induction of cytokine mRNAs in mice after oral exposure to the trichothecene vomitoxin (deoxynivalenol): Relationship to toxin distribution and protein synthesis inhibition. *Toxicol. Appl. Pharmacol.* **133,** 109–120.

Bae, H., Gray, J. S., Li, M., Vines, L., Kim, J., and Pestka, J. J. (2010). Hematopoietic cell kinase associates with the 40S ribosomal subunit and mediates the ribotoxic stress response to deoxynivalenol in mononuclear phagocytes. *Toxicol. Sci.* **115,** 444–452.

Banerjee, S., An, S., Zhou, A., Silverman, R. H., and Makino, S. (2000). RNase L-independent specific 28S rRNA cleavage in murine coronavirus-infected cells. *J. Virol.* **74,** 8793–8802.

Bulavin, D. V., Saito, S., Hollander, M. C., Sakaguchi, K., Anderson, C. W., Appella, E., and Fornace, A. J., Jr (1999). Phosphorylation of human p53 by p38 kinase coordinates N-terminal phosphorylation and apoptosis in response to UV radiation. *EMBO J.* **18,** 6845–6854.

Chung, Y. J., Zhou, H. R., and Pestka, J. J. (2003). Transcriptional and posttranscriptional roles for p38 mitogen-activated protein kinase in upregulation of TNF-alpha expression by deoxynivalenol (vomitoxin). *Toxicol. Appl. Pharmacol.* **193,** 188–201.

Clemens, M. J., Bushell, M., Jeffrey, I. W., Pain, V. M., and Morley, S. J. (2000). Translation initiation factor modifications and the regulation of protein synthesis in apoptotic cells. *Cell Death Differ.* **7,** 603–615.

Clemens, M. J., and Vaquero, C. M. (1978). Inhibition of protein synthesis by double-stranded RNA in reticulocyte lysates: Evidence for activation of an endoribonuclease. *Biochem. Biophys. Res. Commun.* **83,** 59–68.

Endo, Y., and Tsurugi, K. (1986). Mechanism of action of ricin and related toxic lectins on eukaryotic ribosomes. *Nucleic Acids Symp. Ser.* **17,** 187–190.

Ernst, M., Inglese, M., Scholz, G. M., Harder, K. W., Clay, F. J., Bozinovski, S., Waring, P., Darwiche, R., Kay, T., Sly, P., *et al.* (2002). Constitutive activation of the SRC family kinase Hck results in spontaneous pulmonary inflammation and an enhanced innate immune response. *J. Exp. Med.* **196,** 589–604.

Fuentes-Prior, P., and Salvesen, G. S. (2004). The protein structures that shape caspase activity, specificity, activation and inhibition. *Biochem. J.* **384,** 201–232.

Garcia, M. A., Gil, J., Ventoso, I., Guerra, S., Domingo, E., Rivas, C., and Esteban, M. (2006). Impact of protein kinase PKR in cell biology: From antiviral to antiproliferative action. *Microbiol. Mol. Biol. Rev.* **70,** 1032–1060.

Hartley, M. R., and Lord, J. M. (2004). Cytotoxic ribosome-inactivating lectins from plants. *Biochim. Biophys. Acta* **1701,** 1–14.

Hepworth, S. J., Hardie, L. J., Fraser, L. K., Burley, V. J., Mijal, R. S., Wild, C. P., Azad, R., McKinney, P. A., and Turner, P. C. (2012). Deoxynivalenol exposure assessment in a cohort of pregnant women from Bradford, U.K. *Food Addit. Contam. Part A Chem. Anal. Control Expo. Risk Assess.* **29,** 269–276.

Houge, G., and Doskeland, S. O. (1996). Divergence towards a dead end? Cleavage of the divergent domains of ribosomal RNA in apoptosis. *Experientia* **52,** 963–967.

Houge, G., Doskeland, S. O., Boe, R., and Lanotte, M. (1993). Selective cleavage of 28S rRNA variable regions V3 and V13 in myeloid leukemia cell apoptosis. *FEBS Lett.* **315,** 16–20.

Houge, G., Robaye, B., Eikhom, T. S., Golstein, J., Mellgren, G., Gjertsen, B. T., Lanotte, M., and Doskeland, S. O. (1995). Fine mapping of 28S rRNA sites specifically cleaved in cells undergoing apoptosis. *Mol. Cell. Biol.* **15,** 2051–2062.

Islam, Z., Gray, J. S., and Pestka, J. J. (2006). p38 Mitogen-activated protein kinase mediates IL-8 induction by the ribotoxin deoxynivalenol in human monocytes. *Toxicol. Appl. Pharmacol.* **213,** 235–244.

Islam, Z., Shinozuka, J., Harkema, J. R., and Pestka, J. J. (2009). Purification and comparative neurotoxicity of the trichothecenes satratoxin G and roridin L2 from Stachybotrys chartarum. *J. Toxicol. Environ. Health A* **72,** 1242–1251.

Li, M., Cuff, C. F., and Pestka, J. (2005). Modulation of murine host response to enteric reovirus infection by the trichothecene deoxynivalenol. *Toxicol. Sci.* **87,** 134–145.

Li, M., Harkema, J. R., Cuff, C. F., and Pestka, J. J. (2007). Deoxynivalenol exacerbates viral bronchopneumonia induced by respiratory reovirus infection. *Toxicol. Sci.* **95,** 412–426.

Li, M., and Pestka, J. J. (2008). Comparative induction of 28S ribosomal RNA cleavage by ricin and the trichothecenes deoxynivalenol and T-2 toxin in the macrophage. *Toxicol. Sci.* **105,** 67–78.

Liang, S. L., Quirk, D., and Zhou, A. (2006). RNase L: Its biological roles and regulation. *IUBMB Life* **58,** 508–514.

Michot, B., Hassouna, N., and Bachellerie, J. P. (1984). Secondary structure of mouse 28S rRNA and general model for the folding of the large rRNA in eukaryotes. *Nucleic Acids Res.* **12,** 4259–4279.

Moon, Y., and Pestka, J. J. (2002). Vomitoxin-induced cyclooxygenase-2 gene expression in macrophages mediated by activation of ERK and p38 but not JNK mitogen-activated protein kinases. *Toxicol. Sci.* **69,** 373–382.

Muppidi, J., Porter, M., and Siegel, R. M. (2004). Measurement of apoptosis and other forms of cell death. *Curr. Protoc. Immunol.* (Chapter 3), Unit 3.17, 4–5.

Naito, T., Yokogawa, T., Takatori, S., Goda, K., Hiramoto, A., Sato, A., Kitade, Y., Sasaki, T., Matsuda, A., Fukushima, M., *et al.* (2009). Role of RNase L in apoptosis induced by 1-(3-C-ethynyl-beta-D-ribo-pentofuranosyl)cytosine. *Cancer Chemother. Pharmacol.* **63,** 837–850.

Newton, K., and Dixit, V. M. (2012). Signaling in innate immunity and inflammation. *Cold Spring Harb. Perspect. Biol.* **4**, a006049.

Pandey, M., Bajaj, G. D., and Rath, P. C. (2004). Induction of the interferon-inducible RNA-degrading enzyme, RNase L, by stress-inducing agents in the human cervical carcinoma cells. *RNA Biol.* **1,** 21–27.

Pestka, J. J. (2010). Deoxynivalenol: Mechanisms of action, human exposure, and toxicological relevance. *Arch. Toxicol.* **84,** 663–679.

Shifrin, V. I., and Anderson, P. (1999). Trichothecene mycotoxins trigger a ribotoxic stress response that activates c-Jun N-terminal kinase and p38 mitogen-activated protein kinase and induces apoptosis. *J. Biol. Chem.* **274,** 13985–13992.

Stark, G. R., Kerr, I. M., Williams, B. R., Silverman, R. H., and Schreiber, R. D. (1998). How cells respond to interferons. *Annu. Rev. Biochem.* **67,** 227–264.

Tsygankov, A. Y. (2003). Non-receptor protein tyrosine kinases. *Front. Biosci.* **8,** s595–s635.

Turner, P. C., Hopton, R. P., Lecluse, Y., White, K. L., Fisher, J., and Lebailly, P. (2010a). Determinants of urinary deoxynivalenol and de-epoxy deoxynivalenol in male farmers from Normandy, France. *J. Agric. Food Chem.* **58,** 5206–5212.

Turner, P. C., Ji, B. T., Shu, X. O., Zheng, W., Chow, W. H., Gao, Y. T., and Hardie, L. J. (2011). A biomarker survey of urinary deoxynivalenol in China: The Shanghai Women's Health Study. *Food Addit. Contam. Part A Chem. Anal. Control Expo. Risk Assess.* **28,** 1220–1223.

Turner, P. C., White, K. L., Burley, V. J., Hopton, R. P., Rajendram, A., Fisher, J., Cade, J. E., and Wild, C. P. (2010b). A comparison of deoxynivalenol intake and urinary deoxynivalenol in U.K. adults. *Biomarkers* **15,** 553–562.

Williams, B. R. (1999). PKR; a sentinel kinase for cellular stress. *Oncogene* **18,** 6112–6120.

Williams, B. R. (2001). Signal integration via PKR. *Sci. STKE* **2001,** re2.

Wreschner, D. H., James, T. C., Silverman, R. H., and Kerr, I. M. (1981). Ribosomal RNA cleavage, nuclease activation and 2-5A(ppp(A2'p)nA) in interferon-treated cells. *Nucleic Acids Res.* **9,** 1571–1581.

Zhou, H. R., Islam, Z., and Pestka, J. J. (2003a). Rapid, sequential activation of mitogen-activated protein kinases and transcription factors precedes proinflammatory cytokine mRNA expression in spleens of mice exposed to the trichothecene vomitoxin. *Toxicol. Sci.* **72,** 130–142.

Zhou, H. R., Islam, Z., and Pestka, J. J. (2005a). Induction of competing apoptotic and survival signaling pathways in the macrophage by the ribotoxic trichothecene deoxynivalenol. *Toxicol. Sci.* **87,** 113–122.

Zhou, H. R., Jia, Q., and Pestka, J. J. (2005b). Ribotoxic stress response to the trichothecene deoxynivalenol in the macrophage involves the SRC family kinase Hck. *Toxicol. Sci.* **85,** 916–926.

Zhou, H. R., Lau, A. S., and Pestka, J. J. (2003b). Role of double-stranded RNA-activated protein kinase R (PKR) in deoxynivalenol-induced ribotoxic stress response. *Toxicol. Sci.* **74,** 335–344.